Parameter-free nonadiabatic correlation-polarization potential for vibrational excitation in electron-molecule scattering: Application to e-N_2 collisions

Hao Feng* and Weiguo Sun†
College of Physics, Sichuan University, Chengdu, Sichuan 610065, People's Republic of China

Michael A. Morrison‡
Department of Physics and Astronomy, The University of Oklahoma, 440 West Brooks Street, Norman, Oklahoma 73019-0225, USA

(Received 17 May 2003; published 24 December 2003)

This paper introduces a correlation-polarization potential for vibrational excitation in electron-molecule scattering. This potential generalizes a recently proposed model for elastic scattering [Bouferguene *et al.*, Phys. Rev. A **59**, 2712 (1999)]. Our potential contains no adjustable parameters and reflects known qualitative dependencies of correlation and polarization effects on the internuclear separation of the target molecule and on the position coordinate of the scattering electron. We test our potential on vibrationally elastic and inelastic scattering from N_2 in an energy range that includes the $^2\Pi_g$ shape resonance. This resonance gives rise to intricate oscillatory structures in integral and differential cross sections; these structures are very sensitive to the correlation effects this potential is designed to model. Our e-N_2 cross sections agree well with experimental and other theoretical cross sections except at energies above the resonance, where experimental differential cross sections show a pronounced dip at scattering angles below about 60°. This dip is not present in the theoretical cross sections.

DOI: 10.1103/PhysRevA.68.062709 PACS number(s): 34.80.Bm

I. INTRODUCTION

A major practical and conceptual challenge to the theoretical study of low-energy electron scattering from atoms and molecules is the inherently many-body nature of the Schrödinger equation for these systems. Except in the asymptotic region, where the scattering electron is detected, this electron is indistinguishable from target electrons. This quantum-mechanical feature has two consequences, both of which come into play when the scattering electron is inside the target charge cloud. First, the system wave function must be antisymmetric under pairwise electron interchange; this requirement gives rise to ''exchange effects'' on cross sections. Second, instantaneous electron-electron Coulomb interactions render the independent particle model invalid. This many-body aspect of the electron-target system gives rise to ''correlation effects.''

The quantum-mechanical requirement that all electrons must be treated equitably prohibits formal partitioning of the electron-target interaction potential $V_{\rm int}$ into a sum of single-interaction terms. Nevertheless, an approximate partitioning is a useful guide to devising practical strategies for scattering calculations and to understanding the physics implied by the resulting cross sections. This partitioning is especially useful in formulations that transform the many-electron-scattering equation into sets of coupled single-particle equations. In these equations, exchange and correlation effects appear as a nonlocal, energy-dependent optical potential. Thus one often discusses three ''contributions'' to the interaction potential energy: the static, exchange, and correlation-polarization terms [1,2]:

$$V_{\rm int} = V_{\rm st} + V_{\rm ex} + V_{\rm cp}. \tag{1}$$

The static term $V_{\rm st}$ arises from Coulomb interactions between the projectile and the constituents of the target. The exchange term $V_{\rm ex}$ arises from the antisymmetrization requirement. The correlation-polarization term $V_{\rm cp}$ arises from many-body correlation and induced polarization effects. The correlation contribution to $V_{\rm cp}$ is a manifestation of *short-range* bound-free electron-electron correlations. The polarization contribution is a manifestation of *intermediate- and long-range*-induced polarization effects that come into play outside the target charge cloud. At energies below about 20 eV, all three terms in Eq. (1) significantly influence electron-scattering cross sections and must somehow be incorporated in any theoretical method.

During the past few decades, great progress has been made towards accurate treatment of all three contributions in Eq. (1). Inclusion of electrostatic effects by averaging the Coulomb potential energy over a Hartree-Fock probability density for the target is routine [3,4]; more accurate (e.g., configuration interaction) target densities can be used if necessary [5]. One can include exchange effects at various levels of rigor depending on the complexity of the system, the availability of computational resources, and the required accuracy of the desired scattering quantities. For example, exchange can be treated rigorously via solution of the nonlocal coupled integro-differential equations that result from the action of the antisymmetrization operator [6], via basis set expansions in which the nonlocal exchange potential is approximated by a separable expansion [7–9] or via a variety of well-established local model potentials [10–13]. Arguably

*Electronic address: ddsteed@computermail.net
†Electronic address: wgsun@mail.sc.cninfo.net
‡Electronic address: morrison@mail.nhn.ou.edu

the most difficult of these contributions to include accurately is the correlation-polarization term V_{cp}, the focus of the present research.

The easy part of V_{cp} is the intermediate- and long-range polarization potential. One can understand this second-order (induced) interaction via a semiclassical picture. In this picture, the polarization potential is the decrease in the total energy of the system due to the fact that the scattering electron interacts with a target that has been polarized by the electric field of this electron. Outside the target charge cloud, the (local) velocity of the projectile is low enough such that the bound electrons respond *as though the projectile were fixed in space*. Here the projectile's motion can be treated *adiabatically* in calculations of the polarization potential. Asymptotically, the resulting adiabatic polarization potential reduces to a well-known analytic form that contains the polarizability tensor of the target.

Proper quantum-mechanical treatment of correlation and polarization effects is formally straightforward but impossible to implement without approximation. Within the context of eigenfunction-expansion methods, one can treat correlation and polarization effects rigorously by expanding the system wave function in the complete set of (Born-Oppenheimer) target electronic wave functions, including *all* bound and continuum states. In the resulting coupled scattering equations, virtual excitations of energetically inaccessible (closed) target electronic states give rise asymptotically to the polarization potential [14]. If desired, one can dump this infinity of closed states into an optical potential. Unfortunately, the optical potential is energy dependent, nonlocal, and, at scattering energies above the first electronically inelastic threshold, complex. Approximations are mandatory, and a variety of approximate treatments have been explored in recent years [15]. In the widely used class of variational scattering theories—which include the *R*-matrix, Schwinger multichannel, and complex Kohn methods—virtual excitations are incorporated by including configuration state functions in the trial wave function of the electron-molecule system [16–21]. An alternative gambit is to encapsulate this infinity of states in a few deftly chosen pseudostates [22,23].

Notwithstanding their appeal, such potentially rigorous treatments make exceptional computational demands, require great skill in choosing the excited states (or pseudostates), and introduce a problem of correlation balance. In any such approach, whether or not one explicitly invokes an optical potential, one must ensure a consistent treatment of bound-bound correlation (amongst electrons in the target) and bound-free correlation; an imbalance of these two types of correlation can lead to wildly inaccurate results, as has been demonstrated in Refs. [15,18].

All of these difficulties become much more acute if the target contains a large number of electrons and/or is nonlinear. Additional problems arise if the scattering process of interest is a rearrangement process such as dissociative attachment [24] or vibrational excitation, both of which entail significant nonadiabatic energy transfer between the energy of the projectile and the target.

One can make the problem even harder by focusing on resonant scattering. At near-resonant energies, the greatly increased collision time enhances the effects of exchange and correlation on cross sections. Among vibrational excitations, the most sensitive to correlation effects are ''intermediate duration'' resonances such as the $^2\Pi_g$ shape resonance in e-N_2 scattering [25–30]. Although the energy of this resonance is about 2.4 eV, its influence dominates scattering at energies from about 1.5 to 4.0 eV [31]. At these energies, the delicate interplay of projectile and vibrational dynamics induces dense, complicated oscillations in vibrationally elastic $(0\rightarrow 0)$ and inelastic $(0\rightarrow v)$ cross sections. Not only the resonance energy and width but also the particulars of these oscillatory structures depend critically on the short-range electron-molecule interaction. Because of this heightened sensitivity, resonant vibrational excitation of such a system is a particularly challenging test case for theory [32].

The cornucopia of difficulties posed by correlation effects has spawned searches for alternative approaches that seek to mimic these many-body effects via a local model potential. Such strategies strive to treat the local, adiabatic polarization potential that prevails outside the target as accurately as possible, and to incorporate short-range many-electron correlation approximately via a physically motivated *ansatz*. Ideally, such model potentials should be founded on defensible theoretical approximations and free of parameters that would have to be determined from experimental cross sections.

Early model potentials in this class allowed (crudely) for correlation effects by multiplying the known asymptotic form of the polarization potential by a parameter-dependent, spherical cutoff function that weakened the asymptotic potential in the near-target region [33]. More recently, advances in the polarized-orbital method have led to potentials based on the nonpenetrating approximation [34], which implements the extreme but effective expedient of ''switching off'' the bound-free electron-electron Coulomb interaction whenever the radial coordinate of the projectile is less than that of any of the bound electrons. The resulting model potential contains no adjustable parameters and, for systems on which it has been tested, gives cross sections in good-to-excellent agreement with results from experiment and more rigorous theory. In electron-molecule scattering, Gibson and Morrison [35,36] developed this philosophy into the ''better-than-adiabatic dipole (BTAD) potential,'' the calculation of which entails linear variational calculations on the electron-molecule system in the field of a fixed projectile [36,37]. The BTAD potential has been used successfully in calculations of resonant and nonresonant elastic, rotational, and rovibrational cross sections for low-energy electron impact on molecular hydrogen and nitrogen [36,38–43]. Although far less demanding computationally than, say, calculations based on coupled electronic states or an accurate optical potential, computation of the BTAD potential is somewhat awkward because the nonpenetrating approximation forces truncation of electron-electron matrix elements at a finite upper radial limit. Moreover, this approximation, while intuitively appealing, is hard to contextualize theoretically.

The final class of widely used model correlation-polarization potentials treats short-range correlation effects via density-functional correlation potentials that were originally derived for the target. First applied to electron-rare-gas

scattering by O'Connell and Lane [44], this strategy was applied to electron-molecule scattering by Norcross and collaborators (see, for example, Ref. [45]). The most extensive use of such potentials has been by Gianturco and collaborators [46–48], who have applied them to an impressive variety of electron-polyatomic systems [49–52].

Density-functional-based correlation-polarization potentials have the advantages of being real, local, independent of the scattering energy, and calculable from the target charge density. They have the disadvantage of being short range and of not joining smoothly to the long-range polarization potential. Hence their construction requires that one artificially join short-range correlation and asymptotic polarization potentials via the introduction of an empirically chosen ''matching radius'' (Ref. [53], and references therein). Finally, studies of the application of such a density-functional correlation-polarization potential to *vibrational* excitation of molecular hydrogen have shown it to yield considerably less accurate results than the BTAD model [31].

Recently, Bouferguene *et al.* [54] introduced a new model correlation-polarization potential that incorporates bound-free correlation in a way that is distinctly different from all the approaches discussed thus far. Their initial application of this model was to elastic scattering from molecular hydrogen with the internuclear separation fixed at equilibrium. In this application, their correlation-polarization potential involved an adjustable parameter that they determined by matching their potential to the e-H_2 BTAD potential of Gibson and Morrison [36].

We here report a generalization of this model that is free of adjustable parameters and that incorporates known qualitative features of the dependence of correlation effects on the angular position of the scattering electron and on the internuclear separation. To test our model, which we call the *distributed spherical Gaussian* correlation-polarization potential, we have calculated differential and integral cross sections for resonant and nonresonant vibrationally elastic and inelastic e-N_2 scattering.

We commence in Sec. II by reviewing relevant aspects of the potential proposed by Bouferguene *et al.* and describing our generalization of it. We then summarize the scattering theory we used to calculate vibrational excitation cross sections. In Sec. III we compare our integral and differential cross sections for resonant e-N_2 scattering to cross sections from other calculations and from experiment. In Sec. IV we summarize the present work and its implications, and discuss briefly prospects for future related research. Except where noted, we use atomic units throughout this paper.

II. THEORY

A. Adiabatic polarization

In the adiabatic model of polarization, a projectile fixed at $\mathbf{r}_e$ (measured from the center of mass of the target) polarizes the charge distribution of bound target electrons. The mean energy E_0^p of the polarized system, which consists of the scattering electron and the *polarized* target, is lower than the mean energy E_0 of the corresponding unpolarized system. The difference between these two energies is the (attractive) adiabatic polarization potential [55]

$$V^{\mathrm{A}}(\mathbf{r}_e,R)\equiv E_0^p(\mathbf{r}_e,R)-E_0(\mathbf{r}_e,R), \tag{2}$$

where $R\equiv|\mathbf{R}_1-\mathbf{R}_2|$ denotes the internuclear separation. (We consider only diatomic targets.) Quantum mechanically, the energies in this definition are expectation values of the adiabatic (fixed-$\mathbf{r}_e$) electron-molecule Hamiltonian

$$\hat{\mathcal{H}}^{\mathrm{A}}(\boldsymbol{\tau}_e,\mathbf{r}_e,R)\equiv\hat{\mathcal{H}}_m^{\mathrm{e}}(\boldsymbol{\tau}_e;R)+V_{\mathrm{Coul}}(\boldsymbol{\tau}_e,\mathbf{r}_e,R) \tag{3}$$

with respect to the unpolarized and polarized target wave functions ψ_0 and ψ_0^{p}, respectively:

$$E_0(\mathbf{r}_e,R)=\langle\psi_0|\hat{H}^{\mathrm{A}}|\psi_0\rangle_{\tau_e}, \tag{4a}$$

$$E_0^p(\mathbf{r}_e,R)=\langle\psi_0^{\mathrm{p}}|\hat{\mathcal{H}}^{\mathrm{A}}|\psi_0^{\mathrm{p}}\rangle_{\tau_e}. \tag{4b}$$

In these equations, the subscript 0 denotes the ground Born-Oppenheimer electronic state of the target, which for the (unpolarized) N_2 molecule is $X^1\Sigma_g^+$. The symbol $\boldsymbol{\tau}_e$ denotes the coordinates of all bound electrons and appears as a subscript on the expectation values in Eqs. (4) to signify integration over all these coordinates. The two terms in the adiabatic Hamiltonian (3) are the Born-Oppenheimer electronic Hamiltonian $\hat{\mathcal{H}}_m^{\mathrm{e}}$ of the target and the electrostatic Coulomb potential energy V_{Coul}. If the target consists of N_e electrons and N_n nuclei with charges Z_n, then the Coulomb potential energy is

$$V_{\mathrm{Coul}}(\boldsymbol{\tau}_e,\mathbf{r}_e,R)=\sum_{i=1}^{N_e}V_{\mathrm{ee}}(|\mathbf{r}_e-\mathbf{r}_i|)+\sum_{n=1}^{N_n}V_{\mathrm{en}}(|\mathbf{r}_e-\mathbf{R}_n|), \tag{5a}$$

where (in atomic units) the electron-electron and electron-nucleus terms are

$$V_{\mathrm{ee}}(|\mathbf{r}_e-\mathbf{r}_i|)=\frac{1}{|\mathbf{r}_e-\mathbf{r}_i|}, \tag{5b}$$

$$V_{\mathrm{en}}(|\mathbf{r}_e-\mathbf{R}_n|)=-\frac{Z_n}{|\mathbf{r}_e-\mathbf{R}_n|}. \tag{5c}$$

These, of course, are the Coulomb potential energies of interaction between the scattering electron (at $\mathbf{r}_e$) and the bound electrons ($\mathbf{r}_i$) and the nuclei ($\mathbf{R}_n$)—*all treated as point particles*. All coordinates are defined in a body-fixed reference frame with the z axis along the internuclear axis; these coordinates are measured with respect to the center of mass of the molecule.

The purely *adiabatic* polarization potential (2) neglects two important effects. First, the projectile is not actually fixed; rather, it moves with a ''local velocity'' that increases as it nears the target and feels the strong electrostatic attraction of the nucleus. Hence at small to intermediate values of r_e, polarization becomes a dynamic, rather than a static, phenomenon. In the semiclassical picture, we imagine that as the scattering electron nears the target, its speed becomes so

TABLE I. Spherical and nonspherical polarizabilities for N_2 averaged over the ground vibrational state. The BTAD and DSG values were extracted from the respective correlation-polarization potentials at $r_e = 10a_0$. Experimental values are from the work of Newell and Baird [75] and Orcutt and Cole [76] for the spherical polarizability and from the work of Miller and Bederson [77] for the nonspherical polarizability. Structure theory values are from the configuration interaction (CI) calculations of Langhoff *et al.* [74] and coupled-cluster (CC) calculations of Maroulis [57].

	α_0 (a_0^3)	α_2 (a_0^3)
Experiment	11.744 ± 0.004	3.08 ± 0.002
BTAD potential	10.980	3.09
DSG potential	11.369	3.58
Structure theory (CI) [74]	11.616	3.1103
Structure theory (CC) [57]	11.7709	3.0716

large that the bound target electrons can no longer respond *instantaneously* to changes in the electric field produced by the scattering electron. Near the target, therefore, the induced polarization potential should depend on the velocity of the electron as well as its position $\mathbf{r}_e$. (The higher the incident kinetic energy of the electron, the more important is this velocity dependence.) Second, for values of r_e comparable to or smaller than the ''size'' of the target, indistinguishability of the N_e+1 electrons in the system causes the adiabatic approximation, which singles out the projectile as fixed and therefore distinguishable, to break down completely. As the scattering electron *enters* the target charge cloud, bound-free correlation effects become important. Their neglect renders the adiabatic polarization potential far too strong at short- and intermediate-electron coordinates r_e.

As the electron *leaves* the target charge cloud, with r_e increasing to values larger than a few bohr, the adiabatic approximation of Eq. (2) becomes quite accurate. *Asymptotically*, as $r_e \to \infty$, the adiabatic polarization potential reduces to its analytic asymptotic form

$$V^{\mathrm{A}}(\mathbf{r}_e, R) \underset{r_e \to \infty}{\sim} -\frac{\alpha_0(R)}{2r_e^4} - \frac{\alpha_2(R)}{2r_e^4} P_2(\cos\theta_e), \tag{6}$$

where $\alpha_0(R)$ and $\alpha_2(R)$ are the spherical and nonspherical polarizabilities of the target, θ_e is the (body-frame) polar angle of the scattering electron with respect to the internuclear axis, and $P_2(\cos\theta_e)$ is the Legendre polynomial of order 2. (In practice, the value of r_e at which this form accurately represents the polarization potential depends strongly on the target; for small diatomic molecules, $r_e \gtrsim 10a_0$ is typical [56].) In the asymptotic region, theoretically calculated polarization potentials can touch base with reality, through measured values of the averages of $\alpha_0(R)$ and $\alpha_2(R)$ over the ground vibrational state and of the first derivatives of these polarizabilities with respect to R (see Table I below and the discussion and references in Ref. [57]).

B. The spherical Gaussian correlation-polarization potential

The innovation introduced by Bouferguene *et al.* [54] is to model *the scattering electron*, which in the adiabatic polarization potential is a fixed point charge, by a spherical charge density that decays with radial distance from $\mathbf{r}_e$. In their model, the rate of decay of this charge distribution depends linearly on r_e in such a way that as the electron approaches the target ($r_e \to 0$) the density becomes increasingly diffuse, while as the electron leaves the target ($r_e \to \infty$) the density becomes increasingly localized around $\mathbf{r}_e$.

Explicitly, Bouferguene *et al.* proposed a *spherical Gaussian charge density* of the form

$$\rho(\mathbf{r}) = -\left(\frac{2\xi}{\pi}\right)^{3/2} e^{-2\xi|\mathbf{x}-\mathbf{r}_e|^2}, \tag{7}$$

where $\mathbf{r} \equiv \mathbf{x} - \mathbf{r}_e$ is a source point defined relative to the position of the electron $\mathbf{r}_e$ in the body frame and $\mathbf{x}$ is the same point defined relative to the origin of the body frame. This density is normalized to correspond to a total charge of -1 (in atomic units). The exponential factor ξ depends on the *radial* coordinate of the scattering electron as

$$\xi = \beta r_e. \tag{8}$$

To ensure that the exponent in Eq. (7) is dimensionless, β must have dimensions of inverse length cubed. In their application to fixed-nuclei e-H_2 scattering at the equilibrium internuclear separation, Bouferguene *et al.* treated β as a semiempirical parameter, considering values from $0.1 \leqslant \beta \leqslant 0.5$ [79].

To implement this model, one modifies the Coulomb potential energy (5) by replacing the elementary electron charge of the projectile ($e \to -1$ in atomic units) by the charge density $\rho(\mathbf{r})$ to obtain

$$\overline{V}_{\mathrm{Coul}}(\boldsymbol{\tau}_e, \mathbf{r}_e, R) = \sum_{i=1}^{N_e} \overline{V}_{\mathrm{ee}}(|\mathbf{r}_e - \mathbf{r}_i|) + \sum_{n=1}^{N_n} \overline{V}_{\mathrm{en}}(|\mathbf{r}_e - \mathbf{R}_n|), \tag{9}$$

where the electron-electron and electron-nuclei electrostatic potentials due to $\rho(\mathbf{r})$ are

$$\overline{V}_{\mathrm{ee}}(|\mathbf{r}_e - \mathbf{r}_i|) \equiv \int \frac{\rho(\mathbf{r})}{|\mathbf{r}_e - \mathbf{r}_i|}\, d\mathbf{x}, \tag{10a}$$

$$\overline{V}_{\mathrm{en}}(|\mathbf{r}_e - \mathbf{R}_n|) \equiv -\int \frac{\rho(\mathbf{r})}{|\mathbf{r}_e - \mathbf{R}_n|}\, d\mathbf{x}. \tag{10b}$$

[Throughout this paper we use an overbar to signify quantities calculated using the Gaussian charge density (7).] As the radial coordinate of the projectile $r_e \to \infty$ (i.e., as the Gaussian exponent $\xi \to \infty$), Eqs. (10) reduce to the potential energies (5) for point charges. For smaller r_e these potential energies are *weaker* than those of their point-charge counterparts. Moreover, as $|\mathbf{r}_e - \mathbf{r}_i| \to 0$ and $|\mathbf{r}_e - \mathbf{R}_n| \to 0$, these potential energies approach finite constants. In these respects,

the potential of Bouferguene *et al.* effectively mirrors qualitative aspects of electron-electron correlation effects in molecules [59–61].

The modified electrostatic potential energy $\overline{V}_{\mathrm{Coul}}$ is used in place of V_{Coul} in the calculation of the polarized and unpolarized system energies of Eqs. (4). In practice, evaluation of these energies reduces to the evaluation of matrix elements of $\overline{V}_{\mathrm{Coul}}$ in the basis used to expand the polarized (and unpolarized) molecular orbits of the target [36]. Using Gaussian basis functions greatly facilitates evaluation of the required matrix elements [54]. The correlation-polarization potential is then calculated by subtraction as

$$\overline{V}_{\mathrm{cp}}(\mathbf{r}_e,R)=\overline{E}_0^p(\mathbf{r}_e,R)-\overline{E}_0(\mathbf{r}_e,R). \tag{11}$$

The role of the quantity β is now clear: it controls the rate at which the charge density goes to zero as $r=|\mathbf{x}-\mathbf{r}_e|$ increases from $r=0$ at $\mathbf{r}_e$. As β is decreased, the charge density of the scattering electron becomes less concentrated (more diffuse) around $\mathbf{r}_e$; this weakens the correlation-polarization potential. Because the Gaussian exponent $\xi \propto r_e$, this effect is greatest for small r_e (near the target); as r_e increases, the weakening of the correlation-polarization potential diminishes until, in the $r_e\rightarrow\infty$ limit, the projectile is again a point electron moving adiabatically in the field of the (polarized) molecule. In the limit, then, the model correlation-polarization potential (11) reduces to the asymptotic limit (6) of the adiabatic potential (2).

C. A parameter-free distributed spherical Gaussian potential

The model correlation-polarization potential of Bouferguene *et al.* [54] offers several advantages over model potentials based on the nonpenetrating approximation. Most importantly, the integrals required to evaluate this potential are not cut off. Moreover, these integrals entail Gaussian functions and so can easily be evaluated using quantum chemistry codes [59,62]. In application, however, the model proposed by Bouferguene *et al.* suffers from two disadvantages.

First, the quantity β is an *adjustable* parameter. In their studies of e-H_2 scattering, Bouferguene *et al.* chose a value for β to make their potential qualitatively resemble the BTAD model for this system [36]. Moreover, their calculated cross sections showed considerable sensitivity to β: no value of this parameter produced accurate cross sections over the energy range they studied. The problem of treating β as an adjustable parameter becomes more acute when no BTAD potential is available or when vibrational motion is taken into account.

Second, β does not depend on the internuclear separation R or on the scattering angle θ_e. This problem is exacerbated for scattering from targets that are more anisotropic than H_2, especially when the scattering dynamics become more complicated—as in vibrational excitation of N_2. In such cases, both the long- and short-range aspects of the correlation-polarization potential should depend on R and θ_e [31,59,60].

At long range, the extent to which the molecule is polarizable depends on its internuclear geometry. This dependence is easily seen in the fundamental properties of the target; e.g., it appears in the R dependence of the spherical and nonspherical polarizabilities [63] in Eq. (6), and is reflected in all polarization potentials, including the adiabatic potential (2). Moreover, the polarizability of the target and the corresponding potentials depend on the ''angle of approach'' of the projectile. This dependence on θ_e is evident in the strong difference between the parallel and perpendicular polarizabilities and in the corresponding adiabatic potentials [36]. The extremes of this dependence appear when the projectile's incident wave vector is along the internuclear axis (''parallel approach'') or normal to this axis (''perpendicular approach''): the polarization potential for the parallel approach is *much* stronger than for the perpendicular approach.

At short range, the R and θ_e dependencies of correlation and polarization effects are equally important. The qualitative dependence of electron-electron correlation effects on these variables is known from molecular structure calculations (see Vol. 2 of Ref. [60], and references therein) (see also Chaps. 5, 7, and 15 of Ref. [59], and references therein). First, because of the highly anisotropic nature of the target charge distribution, bound-free correlation effects depend on θ_e: e.g., the correction to the adiabatic polarization potential should be different for the parallel approach than for the perpendicular approach. Second, as R increases, the anisotropic target charge distribution encompasses more of space. Therefore corrections to the adiabatic potential to allow for bound-free correlation should depend on R. These dependencies are incorporated into the BTAD potential via the nonpenetrating approximation. In our generalization of the potential of Bouferguene *et al.* [54], we introduce them by making β a function of θ_e and R.

To devise a correlation-polarization potential V_{cp} whose dependence on R and θ_e reflects these properties, we established three criteria. First, as R increases, β should decrease. This criterion ensures that as R increases, the projectile charge distribution will become more diffuse, strengthening V_{cp}. Second, as θ_e decreases, β should decrease. This criterion ensures that V_{cp} is strongest for the parallel configuration and that V_{cp} becomes less attractive as θ_e increases towards the perpendicular configuration. Third, β should reflect the size of the target molecule. After testing several functional forms for $\beta(\theta_e,R)$ to enforce these criteria, we settled on a function that enforces the first criterion by being proportional to $1/R$, the second by depending on the scattering angle as $(1+\sin\theta_e)$, and the third by depending on the equilibrium internuclear separation R_{eq} of the target. The value of R_{eq} is not subject to adjustment; once a target is chosen, its value is fixed, e.g., from tables of spectroscopic data or *ab initio* structure calculations.

The following functional form for $\beta(\theta_e,R)$ satisfies these criteria, is simple analytically, and was the most successful at producing accurate vibrational cross sections:

$$\beta(\theta_e,R)\equiv\frac{1}{RR_{\mathrm{eq}}^2}(1+\sin\theta_e). \tag{12}$$

With this definition, the electron-electron (and electron-nuclei) Coulomb potentials in Eqs. (10) depend on the dis-

tance between $\mathbf{r}_e$ and $\mathbf{r}_i$ (or between $\mathbf{r}_e$ and $\mathbf{R}_n$) and on r_e, θ_e, and R, through the dependence on these variables of the exponential factor

$$\xi(r_e,\theta_e,R)=\beta(\theta_e,R)r_e=\frac{r_e}{RR_{\rm eq}^2}(1+\sin\theta_e). \qquad (13)$$

The factor of $1/R_e^2$ ensures that β is species dependent and dimensionally correct. We shall call this generalization the distributed spherical Gaussian (DSG) potential [80].

Evaluation of the DSG potentials in Eq. (10) is straightforward. Evaluating integrals over spherical Gaussians is a standard part of evaluating one- and two-electron molecular integrals in electronic structure calculations based on Gaussian-type orbital basis functions (see Chap. 9 of Ref. [59]). In particular, the integrals we must evaluate are just Coulomb-interaction integrals over Gaussian distributions. For example, to evaluate $\overline{V}_{\rm ee}(|\mathbf{r}_e-\mathbf{r}_i|)$ we first write $1/r_i$ as an integral over a Gaussian function, then invoke the Gaussian product rule to reduce the result to the one-dimensional integral [62]

$$\overline{V}_{\rm ee}(|\mathbf{r}_e-\mathbf{r}_i|)=\sqrt{\frac{8\xi}{\pi}}\int_0^1 e^{-2\xi|\mathbf{r}_e-\mathbf{r}_i|^2u^2}du. \qquad (14)$$

The integral in Eq. (14) is the familiar Boys function [see Sec. 9.8 of Ref. [59]] $F_n(\eta)$ of order $n=0$ with the argument $\eta=2\xi|\mathbf{r}_e-\mathbf{r}_i|^2$. This function is related to the incomplete Γ function and thence to the error function

$$\mathrm{erf}(x)\equiv\frac{2}{\sqrt{\pi}}\int_0^x e^{-t^2}dt. \qquad (15)$$

In particular, for order $n=0$, the Boys function is

$$F_0(\eta)=\sqrt{\frac{\pi}{4\eta}}\,\mathrm{erf}(\sqrt{\eta}). \qquad (16)$$

Hence the electron-electron potential energy at $\mathbf{r}_i$ due to $\rho(\mathbf{r})$ is simply

$$\overline{V}_{\rm ee}(|\mathbf{r}_e-\mathbf{r}_i|)=\frac{1}{|\mathbf{r}_e-\mathbf{r}_i|}\,\mathrm{erf}(\sqrt{2\xi}|\mathbf{r}_e-\mathbf{r}_i|). \qquad (17a)$$

Similar machinations for the electron-nucleus potential energy yield

$$\overline{V}_{\rm en}(|\mathbf{r}_e-\mathbf{R}_n|)=-\frac{Z_n}{|\mathbf{r}_e-\mathbf{R}_n|}\,\mathrm{erf}(\sqrt{2\xi}|\mathbf{r}_e-\mathbf{R}_n|). \qquad (17b)$$

Several features of β that are important to the physics of the DSG potential are illustrated in Fig. 1. The corresponding projectile charge distributions are illustrated at various internuclear separations R for fixed scattering angle θ_e in Fig. 2 and at various θ_e for fixed R in Fig. 3.

Figure 1 shows that *as the internuclear separation R increases or the scattering angle θ_e decreases, the quantity β decreases*. As illustrated in Figs. 2 and 3, *this decrease in β causes the DSG charge density to become more diffuse*.

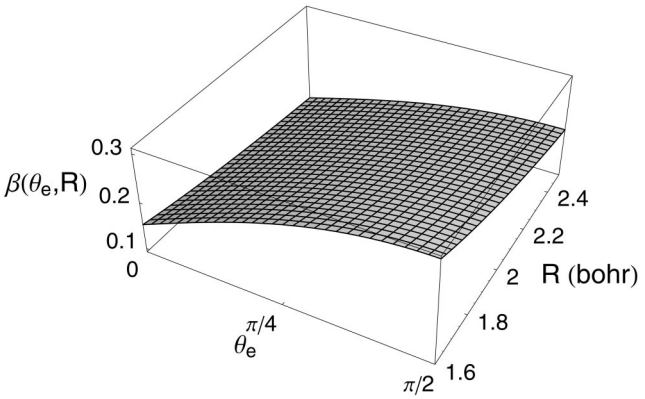

FIG. 1. Dependence on internuclear separation R and scattering angle θ_e of the function $\beta(\theta_e,R)$ in the definition (11) of the distributed charge density for the scattering electron in the DSG potential.

Thus, in this model the correction to the adiabatic polarization potential for bound-free correlation is greater for larger R and/or smaller θ_e. The latter point is especially important: it ensures that (for values of r_e near the target charge cloud) the correction to the adiabatic potential will be greater in the perpendicular configuration ($\theta_e=\pi/2$) than in the parallel configuration ($\theta_e=0$). This point is illustrated in Fig. 3.

D. Scattering theory

In scattering calculations based on a model correlation-polarization potential, the full electron-molecule interaction potential energy in the Schrödinger equation is given by Eq. (1) with the correlation-polarization potential $V_{\rm cp}$ approximated by the DSG potential of Eq. (11). In a previous research on e-N_2 scattering, Sun *et al.* [40] developed a free-electron-gas exchange potential that yielded resonant

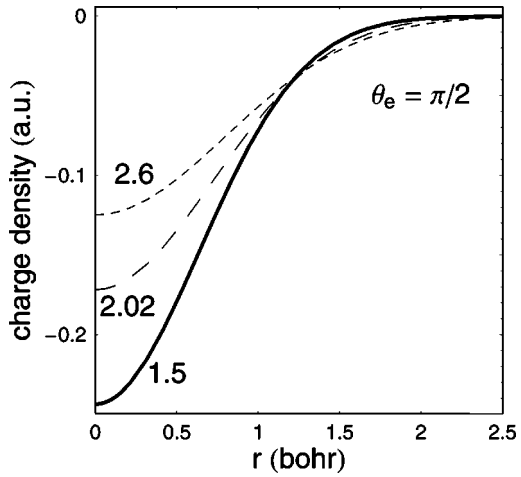

FIG. 2. Charge distributions for the DSG potential for the e-N_2 system as a function of the radial distance r from the scattering electron's coordinate $\mathbf{r}_e$. The radial and angular positions of the scattering electron are fixed at $r_e=2.0a_0$ and $\theta_e=\pi/2$ (perpendicular configuration). Distributions are shown for three internuclear separations $R=1.5a_0$ (solid curve), $2.02a_0$ (dashed curve), and $2.6a_0$ (dotted curve).

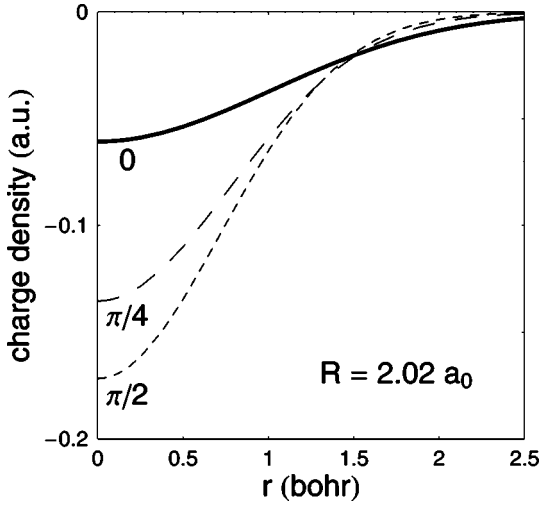

FIG. 3. Projectile charge distributions for the DSG potential for the e-N_2 system as a function of the radial distance r from the scattering electron's coordinate $\mathbf{r}_e$ at fixed internuclear separation $R=2.02a_0$. The radial coordinate of the scattering electron is fixed at $r_e=2.0a_0$. Distributions are shown for the following scattering angles: the parallel configuration $\theta_e=0°$ (solid curve), $\theta_e=\pi/4$ (dashed curve), and the perpendicular configuration $\theta_e=\pi/2$ (dotted curve).

differential cross sections in excellent agreement with data from state-of-the-art crossed-beam experiments. This potential, which has proved equally successful for vibrationally elastic and inelastic excitation of e-H_2 [31,64], is used in the present calculations.

The collision dynamics are treated using the body-frame vibrational close-coupling (BFVCC) method [see Ref. [65], and references therein]. This "hybrid theory" [30,66] is based on the fixed-nuclear-orientation approximation. In this approximation, one neglects the rotational kinetic-energy operator in the system Hamiltonian and allows for target rotation asymptotically, either by averaging over molecular orientations or via the adiabatic nuclear rotation approximation [67–69]. By contrast, the vibrational dynamics of the target are fully incorporated by converging the expansion of the system wave function in vibrational states.

To derive the scattering equations, we first project the electron-molecule Schrödinger equation onto the ground Born-Oppenheimer electronic state of the target. We then expand the resulting scattering function in the complete set $\{\phi_v(R)Y_{\ell,\Lambda}(\hat{\mathbf{r}}_e)\}$, where $\phi_v(R)$ are the vibrational wave functions of the target, and the spherical harmonics $Y_{\ell,\Lambda}(\hat{\mathbf{r}}_e)$ are the angular functions of the scattering electron. The latter are labeled by quantum numbers ℓ for the orbital angular momentum of the projectile and Λ for the projection of this angular momentum on the internuclear axis. In the fixed-nuclear-orientation approximation, Λ is a good quantum number, so the resulting coupled radial equations separate into independent sets for each Λ (and, for a homonuclear target, for each inversion parity). Scattering channels are labeled by $(v,\ell;\Lambda)$.

We can truncate the expansion of the scattering function, retaining a sufficient number N_ℓ^Λ of spherical harmonics and N_v of vibrational states (including closed states if necessary) to converge the cross sections to the desired accuracy. Then we must solve a finite set of $N_v\times N_\ell^\Lambda$ coupled radial scattering equations. Denoting the entrance channel by the subscript 0, we can write these equations as

$$\left[-\frac{1}{2}\frac{d^2}{dr_e^2}+\frac{\ell(\ell+1)}{2r_e^2}+V^\Lambda_{v\ell,v\ell}(r_e)-\frac{1}{2}k_v^2\right]u^\Lambda_{v\ell,v_0\ell_0}(r_e)$$
$$=\sum_{v',\ell'\neq v,\ell}V^\Lambda_{v\ell,v'\ell'}(r_e)u^\Lambda_{v'\ell',v_0\ell_0}(r_e). \tag{18}$$

Here $k_v^2/2$ is the exit-channel energy, determined by energy conservation as

$$\tfrac{1}{2}k_v^2=\tfrac{1}{2}k_0^2-(\epsilon_v-\epsilon_0), \tag{19}$$

where ϵ_v is the energy of the vth vibrational state. The matrix elements of the interaction potential energy,

$$V^\Lambda_{v\ell,v'\ell'}(r_e)=\langle v,\ell;\Lambda|V_{\rm int}|v',\ell';\Lambda\rangle_{R,\hat{\mathbf{r}}_e}, \tag{20}$$

are easily evaluated from the coefficients in an expansion of the interaction potential (at fixed R) in Legendre polynomials,

$$V_{\rm int}(\mathbf{r}_e,R)=\sum_{\lambda=0}^{\infty}{}'\ v_\lambda(r_e,R)P_\lambda(\cos\theta_e), \tag{21}$$

where the prime signifies that for homonuclear targets this sum includes only even values of λ. The Legendre projections $v_\lambda(r_e,R)$ include static, exchange, and correlation-polarization contributions to sufficient maximum order $\lambda_{\max}$ to converge the desired scattering quantities. For comparatively small molecules such as N_2, one need retain only two terms *in the correlation-polarization potential in* $V_{\rm int}$; asymptotically, these terms approach the spherical and nonspherical terms in the analytical form (6). One must retain far more terms in the short-range part of the interaction potential, because the Coulomb potential energy of the scattering electron and the nuclei is strongly anisotropic.

The angular integration in the potential matrix elements (20) is now easily performed using the Gaunt formula, leaving

$$V^\Lambda_{v\ell,v'\ell'}(r_e)=\sum_{\lambda=0}^{\lambda_{\max}}{}'\ g_\lambda(\ell,\ell';\Lambda)w^\lambda_{v,v'}(r_e), \tag{22a}$$

where the angular coupling coefficients, written in terms of Clebsch-Gordan coefficients with the conventions of Rose [70], are simply [65]

$$g_\lambda(\ell,\ell';\Lambda)=\left(\frac{2\ell'+1}{2\ell+1}\right)^{1/2}C(\ell'\lambda\ell;\Lambda 0)C(\ell'\lambda\ell;00). \tag{22b}$$

We evaluate the vibrational coupling matrix elements

$$w^\lambda_{v,v'}(r_e)=\langle\phi_v(R)|v_\lambda(r_e,R)|\phi_{v'}(R)\rangle_R \tag{22c}$$

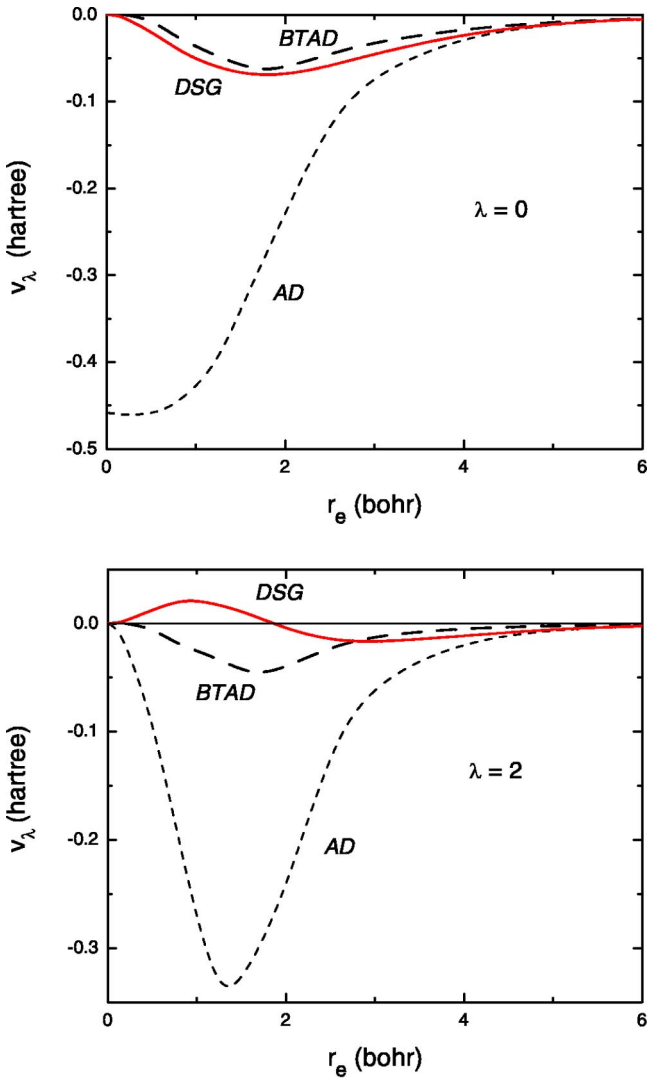

FIG. 4. Spherical (upper) and nonspherical (lower) Legendre projections of the adiabatic (dotted curve), BTAD (dashed curve), and DSG (solid curve) correlation-polarization potentials for the e-N_2 system at $R=2.02a_0$.

by integrating over the internuclear separation R using Morse vibrational wave functions, the parameters of which are given in Ref. [40].

Solution of the coupled radial scattering equations subject to real boundary conditions yields the K matrix from which one can easily determine the corresponding T matrix and thence differential and integral vibrational excitation cross sections; these steps are detailed in Ref. [65]. Because vibrational states are included in the expansion basis, these cross sections explicitly incorporate the dynamic transfer of energy between the projectile and the vibrational degrees of freedom of the target, an effect that is especially important for near-resonant vibrational excitation.

E. Implementation

We calculate the static, exchange, and correlation-polarization potentials from an R-dependent near-Hartree-Fock electronic wave function for the ground state of N_2. A description of the basis used in these calculations, an assessment of the accuracy of the resulting wave functions, and details of the calculation of the static and exchange potentials from these functions appear in Ref. [40].

TABLE II. DSG integral cross sections for vibrationally elastic (σ_{00}) and inelastic (σ_{01}) scattering of electrons from N_2. In the resonance region, energies are chosen to represent the peaks and dips of oscillations in the cross sections. The "grand total" cross sections σ^{tot} are sums of cross sections for all energetically accessible rotational and vibrational excitations.

Energy (eV)	σ_{00} (Å^2)	σ_{01} (Å^2)	$\sigma^{(\mathrm{tot})}$ (Å^2)
0.02	1.609	0	1.609
0.20	5.444	0	5.444
0.55	8.137	0.003	8.140
1.00	9.455	9.455	9.462
1.50	10.858	0.072	10.940
2.00	14.299	3.604	22.872
2.10	16.760	0.821	22.030
2.20	25.837	3.837	34.710
2.30	15.806	5.705	25.544
2.48	26.815	1.480	35.491
2.50	25.575	1.904	33.468
2.70	19.386	4.268	28.180
3.00	17.189	3.543	23.395
3.10	18.303	1.572	22.174
3.20	15.849	1.238	18.804
3.42	15.896	1.214	18.136
4.00	13.593	0.510	14.366
4.50	12.714	0.234	13.029
5.00	12.193	0.129	12.323
6.00	11.632	0.058	11.698
7.00	11.291	0.034	11.328
8.00	11.029	0.023	11.053
9.00	10.801	0.017	10.820
10.00	10.594	0.014	10.609

For the excitations of interest, the vibrational wave functions required to converge the cross sections encompass a range of internuclear distances from $1.60a_0$ to $2.50a_0$ [40]. To construct the coupling matrix elements in Eq. (22c), we evaluated the interaction potential at the following 14 values of R: $1.60a_0$, $1.70a_0$, $1.80a_0$, $1.85a_0$, $1.90a_0$, $1.95a_0$, $2.00a_0$, $2.02a_0$ (the equilibrium internuclear separation for our Hartree-Fock electronic wave function), $2.068a_0$, $2.10a_0$, $2.20a_0$, $2.30a_0$, $2.40a_0$, and $2.50a_0$.

Solution of BFVCC radial equations proceeds via the integral-equations algorithm [65,71], in which we first convert these equations to a set of coupled integral equations, then reduce this set to Volterra form. We solve the resulting equations by numerical propagation from the origin to the asymptotic region, as detailed in Refs. [40,65,72]. The latter reference contains information concerning the convergence of cross sections for this system: number of channels,

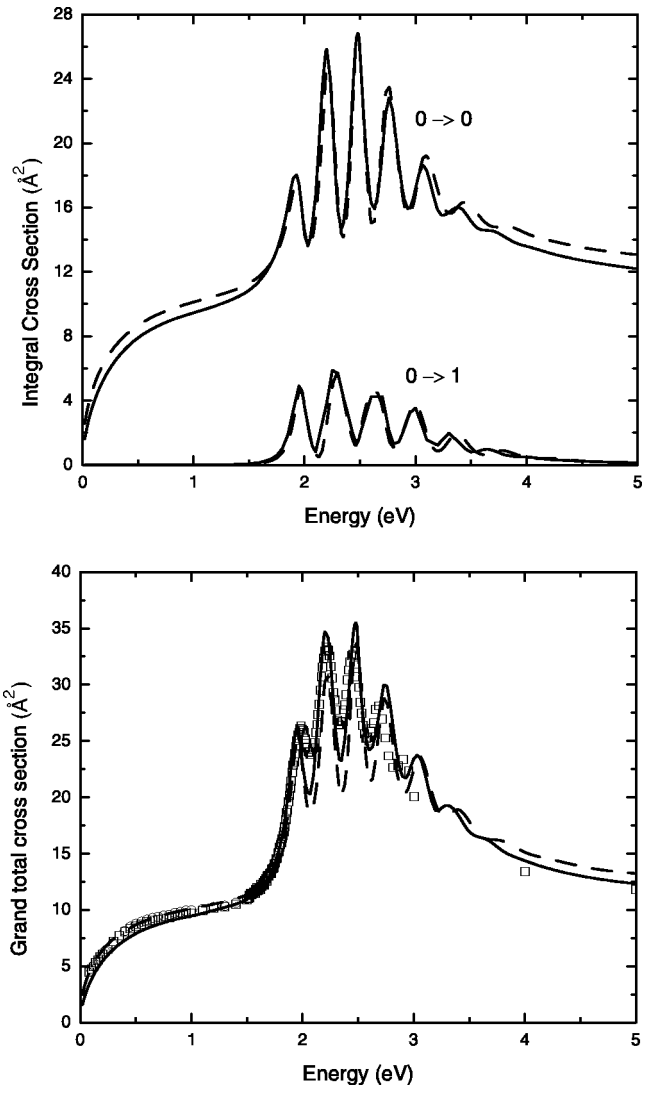

FIG. 5. Integral vibrationally elastic ($0\rightarrow0$) and inelastic ($0\rightarrow1$) (upper) and grand total (lower) e-N_2 cross sections as calculated using the DSG (solid curves) and BTAD (dashed curves) potentials. Experimental grand total cross sections are from crossed-beam (open circles) and time-of-flight (open squares) measurements, as reported by Sun *et al.* [40].

maximum propagation radius, inclusion of Born completion [73] for differential cross sections, etc.

In the solution of these equations considerable savings in CPU time results from exploiting the fact that the electron-molecule interaction potential is severely anisotropic only in the near-target region, where the electron-nuclear electrostatic potential energy dominates. Outside this region one can substantially truncate the solution matrix with no loss of accuracy [33,40,72]. In the present calculations, we used $N_\ell^\Lambda=11$ for $r_e<15.0a_0$ and $N_\ell^\Lambda=3$ from $r_e=15.0a_0$ to $85.0a_0$, at which radius we determined the low-order elements of the K matrix. For $r_e>85.0a_0$, we used Born completion [73] to evaluate additional higher-order elements of the K matrix required to converge the differential cross sections.

TABLE III. Differential cross sections (in square bohr) for vibrational excitation of N_2 as calculated using the DSG correlation-polarization potential.

Angle	$v_0=0\rightarrow v=0$				$v_0=0\rightarrow v=1$	
(deg.)	1.0 eV	1.5 eV	1.9 eV	4.0 eV	2.46 eV	2.60 eV
0	0.598	1.491	9.197	7.936	1.203	3.437
5	0.603	1.449	8.955	8.020	1.182	3.377
10	0.630	1.355	8.301	8.255	1.122	3.202
15	0.704	1.279	7.415	8.580	1.027	2.929
20	0.834	1.280	6.491	8.870	0.906	2.582
25	1.013	1.378	5.659	8.978	0.771	2.193
30	1.219	1.555	4.981	8.800	0.632	1.796
35	1.432	1.785	4.474	8.329	0.501	1.425
40	1.647	2.051	4.146	7.641	0.390	1.109
45	1.867	2.350	4.010	6.843	0.305	0.871
50	2.096	2.679	4.069	6.024	0.252	0.722
55	2.330	3.027	4.306	5.239	0.231	0.665
60	2.561	3.375	4.674	4.520	0.239	0.690
65	2.776	3.695	5.108	3.888	0.270	0.779
70	2.963	3.966	5.534	3.359	0.316	0.908
75	3.118	4.170	5.892	2.941	0.366	1.050
80	3.238	4.300	6.132	2.635	0.412	1.176
85	3.325	4.354	6.224	2.426	0.446	1.266
90	3.377	4.333	6.151	2.298	0.461	1.303
95	3.397	4.240	5.920	2.229	0.455	1.282
100	3.388	4.085	5.556	2.207	0.430	1.207
105	3.354	3.882	5.107	2.217	0.391	1.091
110	3.302	3.648	4.631	2.253	0.343	0.956
115	3.235	3.398	4.191	2.314	0.298	0.828
120	3.157	3.144	3.842	2.404	0.264	0.734
130	2.967	2.660	3.602	2.700	0.263	0.741
140	2.758	2.271	4.141	3.174	0.382	1.094
150	2.578	2.030	5.371	3.800	0.609	1.753
160	2.452	1.921	6.873	4.459	0.876	2.525
170	2.375	1.889	8.095	4.956	1.091	3.144
180	2.348	1.884	8.565	5.138	1.173	3.380

III. RESULTS

A. The DSG correlation-polarization potential

In Fig. 4 we show the spherical and nonspherical Legendre projections [$\lambda=0$ and $\lambda=2$ in Eq. (21)] of the DSG e-N_2 correlation-polarization potential at $R=2.02a_0$. We also compare these functions to the corresponding projections of the adiabatic and BTAD potentials [40]. For projectile coordinates r_e far from the target, the adiabatic, BTAD, and DSG polarization potentials all tend to zero, and the differences between them become negligible. But as r_e decreases and the scattering electron nears the molecule, the adiabatic potential is far stronger than either the BTAD or DSG potentials, especially near the nuclear cusp at $r_e\sim1.0a_0$. Inside the target charge cloud, the BTAD and DSG potentials are weaker than the adiabatic potential and go to zero as $r_e\rightarrow0$, as they should.

In Table I we compare the spherical and nonspherical polarizabilities extracted from our DSG potential with those

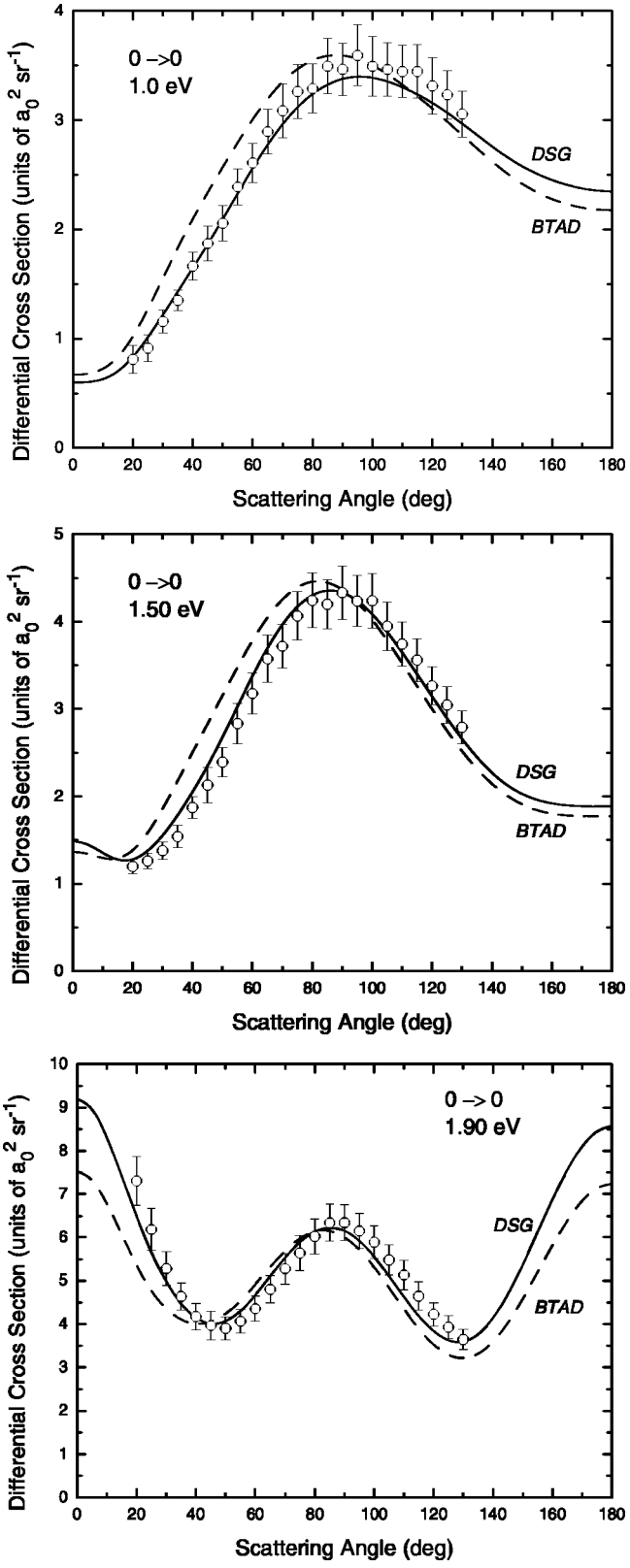

FIG. 6. Resonant vibrationally elastic differential cross sections for e-N_2 scattering at 1.0 eV (top), 1.5 eV (middle), and 1.9 eV (bottom). Theoretical results were calculated using the DSG (solid curve) and BTAD (dashed curve) potentials. Experimental data are from crossed-beam measurements, as reported by Sun *et al.* [40].

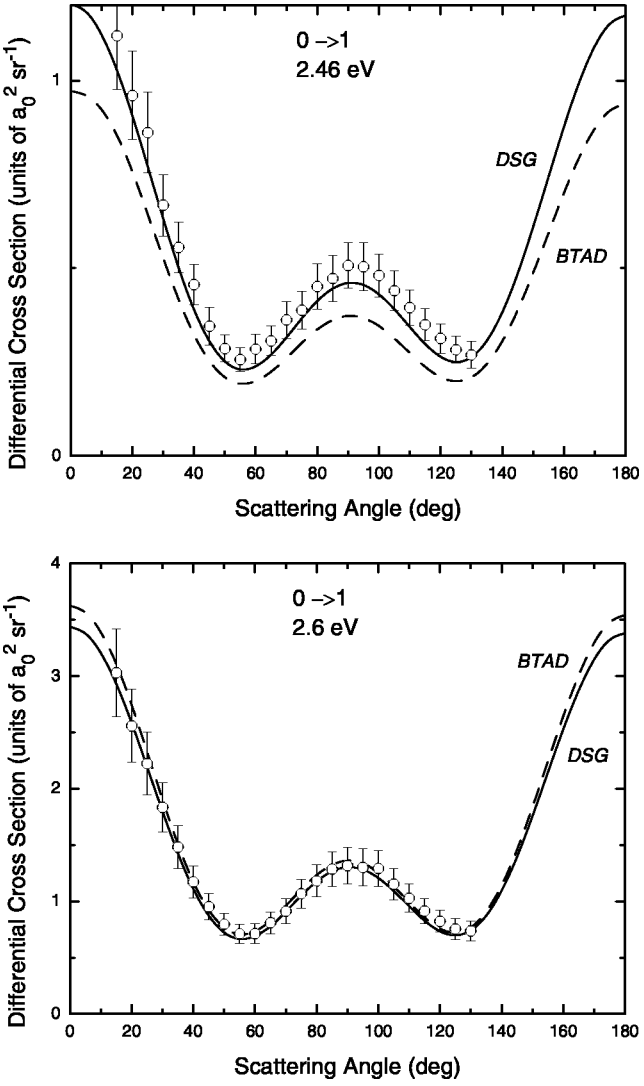

FIG. 7. Resonant vibrationally inelastic $0 \rightarrow 1$ differential cross sections for e-N_2 scattering at 2.46 eV (upper) and 2.6 eV (lower). Theoretical results were calculated using the DSG (solid curve) and BTAD (dashed curve) potentials. Experimental data are from crossed-beam measurements, as reported by Sun *et al.* [40].

from the BTAD potential, from experimental data and from electronic structure theory calculations. [Maroulis [57] has compared recent theoretical calculations of these (and other) properties of N_2 in its ground electronic state.] To enable a meaningful comparison to experiment, we have averaged the theoretical polarizabilities over the ground vibrational state of the target. The DSG spherical polarizability agrees marginally better with the measured value than does the BTAD spherical polarizability, while the DSG nonspherical polarizability is larger than the experimental value. Since $\alpha_0 > \alpha_2$, the spherical polarizability term in the asymptotic form (6) dominates in the long-range region.

B. Integral cross sections

Integral vibrationally elastic and inelastic ($v_0 = 0 \rightarrow v = 1$) cross sections calculated using the DSG potential are tabulated at selected energies in Table II. (A full list of these

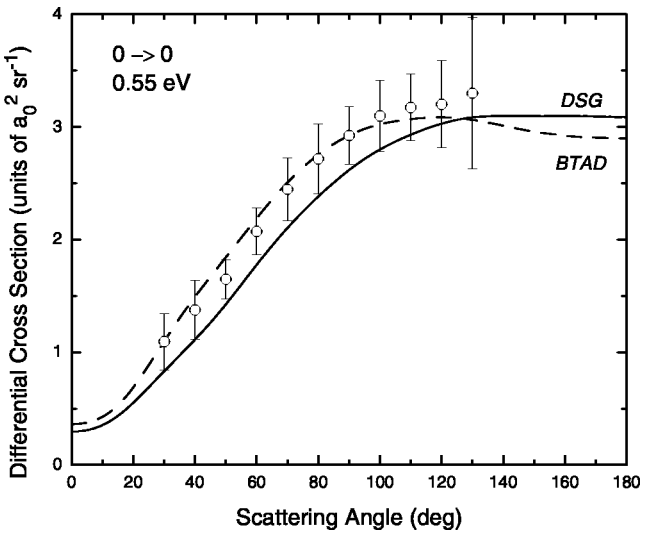

FIG. 8. Nonresonant vibrationally elastic differential cross sections for e-N_2 scattering at 0.55 eV from theoretical calculations using the DSG (solid curve) and BTAD (dashed curve) potentials. Experimental data are from crossed-beam measurements, as reported by Sun *et al.* [40].

data are available from the authors on request.) We compare these cross sections to those from BTAD calculations and from recent crossed-beam and time-of-flight measurements in Fig. 5.

The agreement between integral cross sections calculated with the BTAD and DSG models is striking, especially considering the different ways in which these potentials treat bound-free correlation effects. Both models yield cross sections that agree very well with experimental cross sections, even at energies near the shape resonance, where these cross sections are especially sensitive to correlation effects.

C. Differential cross sections

Differential cross sections (DCS) pose a significantly greater challenge to theory than do their integrated counterparts. So we have calculated e-N_2 DCS for vibrationally elastic ($0\rightarrow0$) and inelastic ($0\rightarrow1$) scattering at several energies, primarily in the resonance region from 1.5 to 4.0 eV. For this system, the nature of nonresonant scattering differs significantly from that of resonant scattering [40]. Hence we also calculated DCS at selected energies below and above the resonance region.

Specifically, in order to facilitate comparison with experiment, we calculated $0\rightarrow0$ DCS at and near the first resonance peak, which occurs at $E_0=1.90$ eV, and $0\rightarrow1$ DCS at and near the resonance peak at $E_0=2.6$ eV (see Table I of Ref. [40]). To illustrate scattering at energies below the resonance, we chose $E_0=0.55$, 1.0, and 1.5 eV. The upper end of the resonance region is about 4.0 eV, so we considered this energy and one clearly above this region, 5.0 eV. Our results for both excitations and several energies at selected energies are tabulated in Table III.

Figure 6 compares resonant $0\rightarrow0$ cross sections from our DSG and BTAD calculations with data from recent crossed-beam experiments [40] at and near the first resonant peak.

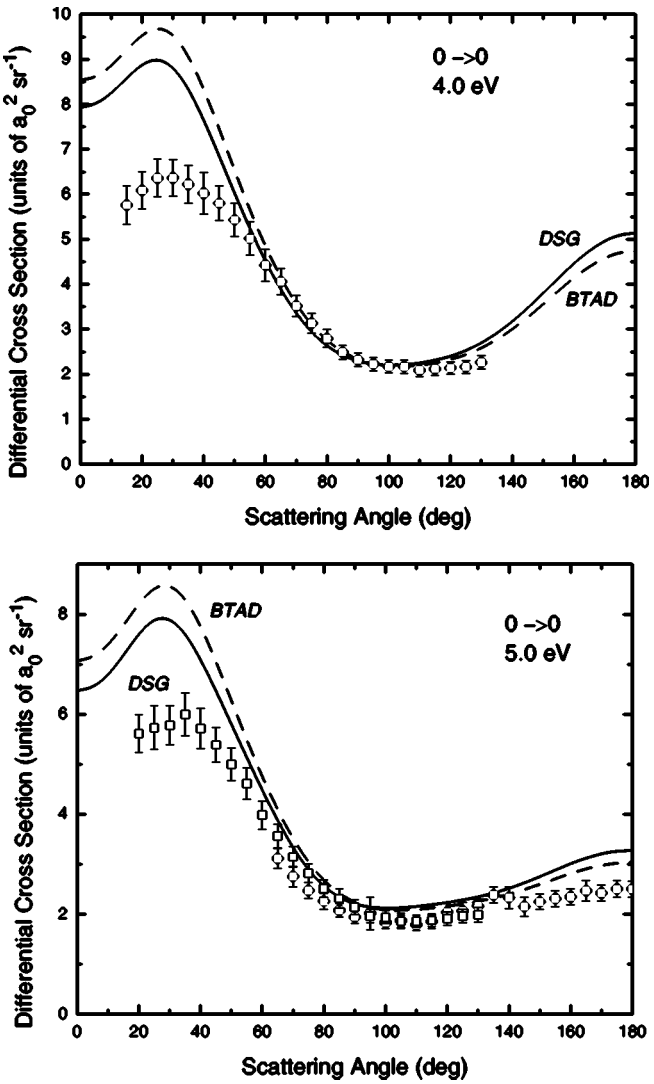

FIG. 9. Nonresonant vibrationally elastic differential cross sections for e-N_2 scattering at 4.0 eV (upper) and 5.0 eV (lower) from theoretical calculations using the DSG (solid curve) and BTAD (dashed curve) potentials. Experimental data are from crossed-beam measurements, as reported by Sun *et al.* [40].

Qualitatively, both theoretical DCS agree with the experimental data; quantitatively, the DSG results are in slightly better agreement with experiment, especially for scattering at 1.9 eV at angles below about 50°. At this energy, *d*-wave scattering clearly dominates the cross section. This dominance is even clearer in the vibrationally inelastic resonant DCS for $E=2.46$ eV and $E=2.60$ eV shown in Fig. 7. The two theoretical DCS are quite close at 2.6 eV, while at 2.46 eV the DSG cross section is marginally larger than its BTAD counterpart, in better agreement with the data.

For nonresonant scattering, we find similar differences between BTAD and DSG cross sections and roughly the same level of agreement with experiment *except at energies above the resonance region*. At energies *below* this region, as illustrated in Fig. 8, the DCS arises mainly from Σ electron-molecule symmetries and show no trace of the resonance shapes seen in Fig. 6.

Something quite different emerges from comparisons of DCS in Fig. 9 at energies *above* the resonance region. At 4.0 and 5.0 eV, at angles less than about 60°, both theoretical DCS are significantly larger than the experimental data. This disagreement is especially unfortunate, since it renders experiment unable to discriminate between the two theoretical models, whose DCS differ from one another only in this angular region. It is noteworthy, however, that at these energies the differences between the two theoretical DCS are not as great as the differences between the theoretical and experimental DCS.

IV. CONCLUSIONS

The goal of this research was to devise a model correlation-polarization potential, building on the work of Bouferguene *et al.*, that is free of adjustable parameters, that reflects qualitatively known properties of correlation and polarization effects from structure and other electron scattering studies, and that is suitable for scattering processes in which changes in the internuclear separation are critical. The distributed spherical Gaussian (DSG) model potential described in Sec. II C satisfies these criteria. In addition, the DSG potential is dimensionally correct. Calculating the DSG potential is computationally efficient, because its functional form is simple and based on Gaussian functions.

The key equations of the DSG model are Eq. (7), which gives the charge density of the scattering electron; Eq. (12), which gives the quantity $\beta(R,\theta_e)$ in this density; and Eq. (11), which shows how to use this density to calculate the correlation-polarization potential. Important qualitative features of this quantity and of the DSG density are illustrated in Figs. 1–3.

Although the ways in which the BTAD and DSG potentials approximate bound-free correlation effects are quite different, the two models give strikingly similar cross sections. No significant differences are evident between the BTAD and DSG integral cross sections in Fig. 5: both models produce results within the error bars of recent crossed-beam and time-of-flight data. Even the DSG and BTAD differential cross sections in Figs. 6–8 manifest only slight differences. In cases where the BTAD and DSG results differ enough such that we can use experimental data to discriminate between them, the DSG cross sections agree marginally better with the data. However, a significant *disagreement* between experimental data and *both* theoretical differential cross sections appears in Fig. 9 above the resonance region at angles less than about 60°. At present we have no explanation for this difference.

Some insight into the success of the DSG potential may be gleaned from the correlation hole formalism of electronic structure theory [59,78]. The modified Coulomb potential of Eqs. (10) successfully mimics three features of the (exact) Coulomb hole about its ''reference point,'' which for electron scattering is the position $\mathbf{r}_e$ of the projectile. First, the DSG charge distribution is localized around this point. Second, this charge distribution follows the reference point as the coordinate of the scattering electron changes. Third, the DSG effective potential is *weaker* than the adiabatic polarization potential. This weakening arises because the assumptions of the DSG model diminish the probability of finding the scattering electron near one of the bound electrons. These assumptions thus mimic ''left-right correlation'' [61].

The accuracy of our integral and differential elastic and vibrational e-N_2 cross sections supports the basic soundness of the DSG model and argues for further investigation of correlation-polarization potentials derived from such models. One can view the DSG charge density of Eq. (12) as a particular example of a general strategy for approximating correlation-polarization effects in electron scattering by modeling the projectile as a distributed density function. The present results warrant exploring such models in studies of vibrational excitation of other molecules and of resonance-driven rearrangement processes such as dissociative attachment. We are therefore currently applying this model to a more diverse range of molecules and scattering processes.

ACKNOWLEDGMENTS

We are grateful to Dr. Andrew N. Feldt for his careful reading of this manuscript and for suggestions that led to its improvement. We would like to acknowledge the Chinese National Natural Science Foundation (Grant No. 10074048) and the Science Foundation of the Chinese Educational Ministry for support of this project. This project was supported in part by the National Science Foundation under Grant No. PHY-0071031.

[1] N. F. Lane, Rev. Mod. Phys. **52**, 29 (1980).
[2] M. A. Morrison, Aust. J. Phys. **36**, 239 (1983).
[3] M. A. Morrison, Comput. Phys. Commun. **21**, 63 (1980).
[4] G. B. Schmid, D. W. Norcross, and L. A. Collins, Comput. Phys. Commun. **21**, 79 (1980).
[5] A. N. Feldt, Phys. Rev. A **37**, 3573 (1988).
[6] W. K. Trail, Ph.D. thesis, University of Oklahoma, 1991 (unpublished).
[7] B. I. Schneider and L. A. Collins, Phys. Rev. A **24**, 1264 (1981).
[8] L. A. Collins and B. I. Schneider, Phys. Rev. A **34**, 1564 (1986).
[9] G. Danby, B. K. Elza, M. A. Morrison, and W. K. Trail, J. Phys. B **29**, 2265 (1996).
[10] M. A. Morrison, L. A. Collins, and N. F. Lane, Chem. Phys. Lett. **42**, 356 (1976).
[11] M. A. Morrison and L. A. Collins, Phys. Rev. A **17**, 918 (1978).
[12] M. A. Morrison and L. A. Collins, Phys. Rev. A **23**, 127 (1981).
[13] L. A. Collins and M. A. Morrison, Phys. Rev. A **25**, 1764 (1982).
[14] L. Castillejo, I. C. Percival, and M. J. Seaton, Proc. R. Soc. London, Ser. A **254**, 259 (1960).

[15] B. I. Schneider and L. A. Collins, Phys. Rev. A **30**, 95 (1984).
[16] *Computational Methods for Electron-Molecule Collisions*, edited by W. M. Huo and F. A. Gianturco (Plenum Press, New York, 1995).
[17] T. N. Rescigno, B. H. Lengsfield III, and C. W. McCurdy, in *Modern Electronic Structure Theory Part*, edited by D. R. Yarkony (World Scientific, River Edge, NJ, 1995), Chap. 9, pp. 501–588.
[18] T. N. Rescigno, in *Supercomputing, Collision Processes, and Applications*, edited by K. L. Bell (Kluwer Academic, Dordrecht/Plenum, New York, 1999), pp. 67–76.
[19] C. Winstead and V. McKoy, Adv. At. Mol. Phys. **43**, 111 (2000).
[20] D. L. Azevedo, A. J. R. da Silva, and M. A. P. Lima, Phys. Rev. A **61**, 042702 (2000).
[21] D. L. Azevedo and M. A. P. Lima, Phys. Rev. A **63**, 062703 (2001).
[22] P. G. Burke and J. F. B. Mitchell, J. Phys. B **7**, 665 (1974).
[23] B. I. Schneider, Chem. Phys. Lett. **51**, 578 (1977).
[24] M. Le Dourneuf, B. I. Schneider, and P. G. Burke, J. Phys. B **12**, L365 (1979).
[25] J. N. Bardsley and F. Mandl, Rep. Prog. Phys. **31**, 471 (1962).
[26] M. Krauss and F. H. Mies, Phys. Rev. A **1**, 1592 (1970).
[27] T. N. Rescigno, A. E. Orel, and C. W. McCurdy, J. Chem. Phys. **73**, 6347 (1980).
[28] A. U. Hazi, T. N. Rescigno, and M. Kurilla, Phys. Rev. A **23**, 1089 (1981).
[29] P. L. Gertitschke and W. Domcke, J. Phys. B **26**, 2927 (1993).
[30] C. A. Weatherford and A. Temkin, Phys. Rev. A **49**, 2580 (1994).
[31] M. A. Morrison and B. C. Saha, Phys. Rev. A **34**, 2786 (1986).
[32] B. I. Schneider, M. Le Dourneuf, and V. K. Lan, Phys. Rev. Lett. **43**, 1926 (1979).
[33] M. A. Morrison, N. F. Lane, and L. A. Collins, Phys. Rev. A **151**, 2186 (1977).
[34] A. Temkin, Phys. Rev. **107**, 1004 (1957).
[35] T. L. Gibson and M. A. Morrison, J. Phys. B **15**, L221 (1982).
[36] T. L. Gibson and M. A. Morrison, Phys. Rev. A **29**, 2497 (1984).
[37] T. L. Gibson, Ph.D. thesis, University of Oklahoma, 1982 (unpublished).
[38] M. A. Morrison, B. C. Saha, and T. L. Gibson, Phys. Rev. A **36**, 3682 (1987).
[39] W. K. Trail, M. A. Morrison, W. A. Isaacs, and B. C. Saha, Phys. Rev. A **41**, 4868 (1990).
[40] W. Sun, M. A. Morrison, W. A. Isaacs, W. K. Trail, D. T. Alle, R. J. Gulley, M. J. Brennan, and S. J. Buckman, Phys. Rev. A **52**, 1229 (1995).
[41] M. T. Elford, R. W. Crompton, M. J. Brennan, M. A. Morrison, W. A. Isaacs, W. Sun, and W. K. Trail, Aust. J. Phys. **50**, 441 (1997).
[42] M. A. Morrison, W. Sun, W. A. Isaacs, and W. K. Trail, Phys. Rev. A **55**, 2786 (1997).
[43] A. G. Robertson, M. T. Elford, R. W. Crompton, M. A. Morrison, W. Sun, and W. K. Trail, Aust. J. Phys. **50**, 441 (1997).
[44] J. K. O'Connell and N. F. Lane, Phys. Rev. A **27**, 1893 (1983).
[45] N. T. Padial and D. W. Norcross, Phys. Rev. A **29**, 1742 (1984).
[46] F. A. Gianturco and J. A. Rodriguez-Ruiz, J. Mol. Struct.: THEOCHEM **260**, 99 (1992).
[47] F. A. Gianturco and J. A. Rodriguez-Ruiz, J. Phys. B **47**, 1075 (1993).
[48] F. A. Gianturco, A. Jain, and J. A. Rodriguez-Ruiz, Phys. Rev. A **48**, 4321 (1993).
[49] F. A. Gianturco and S. Scialla, J. Phys. B **20**, 3173 (1987).
[50] F. A. Gianturco and S. Scialla, J. Chem. Phys. **87**, 6468 (1987).
[51] R. R. Lucchese and F. A. Gianturco, Int. Rev. Phys. Chem. **15**, 429 (1996).
[52] F. A. Gianturco and P. Paioletti, in *Novel Aspects of Electron-Molecule Collisions*, edited by K. H. Becker (World Scientific, Teaneck, NJ, 1998), pp. 57–199.
[53] M. Cascella, R. Curik, and F. A. Gianturco, J. Phys. B **34**, 705 (2001).
[54] A. Bouferguene, I. Ema, and C. A. Weatherford, Phys. Rev. A **59**, 2712 (1999).
[55] R. J. W. Henry and N. F. Lane, Phys. Rev. **173**, 183 (1969).
[56] M. A. Morrison and P. J. Hay, Phys. Rev. A **20**, 740 (1979).
[57] G. Maroulis, J. Chem. Phys. **118**, 2673 (2003).
[58] J. Kobus, H. M. Quiney, and S. Wilson, J. Phys. B **45**, 2045 (2001).
[59] T. Helgaker, P. Jørgensen, and J. Olsen, *Molecular Electronic-Structure Theory* (Wiley, New York, 2000).
[60] *Handbook of Molecular Physics and Quantum Chemistry*, edited by S. Wilson (Wiley, New York, 2003).
[61] R. McWeeny, *Electron Correlation in Molecules* (Ref. [60]), Vol. 2, Chap. 15, pp. 191–197.
[62] T. Helgaker and P. R. Taylor, in *Modern Electronic Structure Theory*, edited by D. R. Yarkony (World Scientific, River Edge, NJ, 1995), pp. 727–760.
[63] M. A. Morrison and P. J. Hay, J. Chem. Phys. **70**, 4034 (1979).
[64] M. A. Morrison, R. W. Crompton, B. C. Saha, and Z. L. Petrovic̀, Aust. J. Phys. **40**, 239 (1987).
[65] M. A. Morrison and W. Sun, in *Computational Methods for Electron-Molecule Collisions*, edited by W. Huo and F. Gianturco (Plenum, New York, 1995), Chap. 6, pp. 131–190.
[66] N. Chandra and A. Temkin, Phys. Rev. A **13**, 188 (1976).
[67] D. M. Chase, Phys. Rev. **104**, 838 (1956).
[68] S. Hara, J. Phys. Soc. Jpn. **27**, 1592 (1969).
[69] A. Temkin and K. V. Vasavada, Phys. Rev. **160**, 109 (1967).
[70] M. E. Rose, *Elementary Theory of Angular Momentum* (Wiley, New York, 1957).
[71] W. N. Sams and D. J. Kouri, J. Chem. Phys. **51**, 4809 (1969).
[72] M. A. Morrison, in *Electron-Molecule and Photon-Molecule Collisions*, edited by T. Rescigno, V. McKoy, and B. I. Schneider (Plenum, New York, 1979).
[73] W. A. Isaacs and M. A. Morrison, Phys. Rev. A **53**, 4215 (1996).
[74] S. R. Langhoff, C. W. B. , Jr., and D. P. Chong, J. Chem. Phys. **78**, 5287 (1983).
[75] A. C. Newell and R. C. Baird, J. Appl. Phys. **36**, 3751 (1965).
[76] R. H. Orcutt and R. H. Cole, J. Chem. Phys. **46**, 697 (1967).
[77] T. M. Miller and B. Bederson, Adv. At. Mol. Phys. **13**, 1 (1978).
[78] A. D. Becke, in *Modern Electronic Structure Theory*, edited by D. R. Yarkony (World Scientific, River Edge, NJ, 1995), pp. 1022–1044.
[79] In spirit, this model is akin to the parametrized spherical dis-

tributed nucleus models such as the Gaussian and Fermi models that have been used to take account of the finite size of the nucleus in electron structure theory of atoms and molecules (Ref. [58] and references therein).

[80] This usage should not be confused with distributed Gaussian basis functions on discretized grids. We use ''distributed'' to refer to the fact that in this model the projectile's charge distribution is ''spread out'' over space and ''Gaussian'' to allude to the use of a Gaussian function in Eq. (7).